Systematic Parameter Optimization for Electrospraying of PVA and PVP Aqueous Solutions

Wilbert Arturo Vivas-Torrez[1], Héctor D. López-Calderón[2], Juan Rodrigo Laguna-Camacho[1,*], Andrea Guadalupe Martínez-López[3], Víctor Velázquez-Martínez[1], Javier Calderón-Sánchez[1], Jesús Enrique López-Calderón[1] and Celia Calderón-Ramón[1]

[1]*Universidad Veracruzana, Facultad de Ingeniería Mecánica y Eléctrica, Poza Rica, Veracruz, Mexico*

[2]*Universidad Veracruzana, Facultad de Biología, Xalapa, Veracruz, Mexico*

[3]*Universidad Veracruzana, Centro de Investigación en Micro y Nanotecnología, Boca del Río, Veracruz, México*

Abstract: This study systematically optimizes the key electrospraying parameters—flow rate, applied voltage, and nozzle-collector distance—for generating polymer micro/nanospheres from aqueous solutions of polyvinyl alcohol (PVA) and polyvinylpyrrolidone (PVP). Solutions at concentrations of 10%–15% w/v were characterized by conductivity measurements, revealing a significant solvent-dependent effect (450 µS/m–590 µS/m for water vs. 44 µS/m–56 µS/m for ethanol). Through iterative testing, two distinct sets of optimal parameters were identified: 10% PVA at 20 µL/h, 25 kV, and 12 cm distance, and 15% PVP at 10 µL/h, 30 kV, and 14 cm distance. Statistical analysis (ANOVA) confirmed a significant interaction between polymer type and concentration on solution conductivity ($p < 0.05$). Strict environmental control (≤24 °C, ≤44% RH) was essential for process stability. Optical microscopy confirmed the formation of structures under the optimized conditions. This work establishes a reproducible parametric framework for the electrospraying of PVA and PVP, providing a critical foundation for the subsequent development of functional polymer particles for potential applications in catalysis and drug delivery.

Keywords: Electrospraying, Parameter Optimization, Polyvinyl Alcohol (PVA), Polyvinylpyrrolidone (PVP), Taylor Cone, Polymer Processing.

1. INTRODUCTION

Electrospraying has emerged as a versatile technique for generating polymer micro- and nanoparticle systems, with applications ranging from biomedicine to environmental remediation [1-3]. The process relies on applying a high electric field to a polymer solution, which leads to Taylor cone formation and the breakup of the jet into charged droplets. Successful electrospraying is governed by multiple interrelated parameters: solution properties (e.g., concentration, conductivity) [4,5]; process conditions (voltage, flow rate, needle-collector distance) [6,7]; and environmental factors (temperature, humidity) [8]. Systematic optimization of these parameters is essential to achieve reproducible morphologies and particle sizes.

Polyvinyl alcohol (PVA) and polyvinylpyrrolidone (PVP) are two widely used water-soluble polymers suitable for electrospraying due to their distinct physicochemical properties. PVA exhibits excellent film-forming ability, high hydrophilicity, and biocompatibility [9,10]. PVP offers broader solvent compatibility (soluble in both water and ethanol) and regulatory approval for various applications [11,12,19]. Both polymers are commonly employed in hydrogel fabrication and have been explored for the development of functional nanostructures [10,12]. However, a direct comparative study systematically optimizing electrospraying parameters for PVA and PVP—particularly for environmental applications—remains lacking.

Previous work has demonstrated the feasibility of electrospraying PVA solutions [13] and the potential of TiO_2-based nanostructures for photocatalytic dye degradation [14, 15]. Nevertheless, establishing a reliable, reproducible parameter window for PVA and PVP electrospraying is a critical prerequisite for advancing toward such functional composite materials. This study addresses this research gap by systematically determining the optimal electrospraying parameters (flow rate, voltage, and distance) for PVA and PVP solutions in different solvents. The findings provide a foundational framework for subsequent development of polymer-based micro/nanospheres, with potential future integration of photocatalytic nanomaterials for wastewater treatment applications.

2. MATERIALS AND METHODS

2.1. Fundamental Concepts

The electrospinning principle central to this work occurs when a liquid droplet anchored at the end of a tube assumes a near-spherical shape due to gravity and surface tension. Under high-intensity electric fields, free charges redistribute to counteract the field,

*Address correspondence to this author at the Universidad Veracruzana, Facultad de Ingeniería Mecánica y Eléctrica, Poza Rica, Veracruz, Mexico; E-mail: jlaguna@uv.mx

E-ISSN: 1929-5995/25

accumulating at the liquid surface. Increasing the potential generates repulsive forces that weaken cohesive surface tension, deforming the meniscus into a conical structure (the Taylor Cone). Beyond a critical threshold, the jet destabilizes into charged droplets.

Electrospraying generates charged droplets by applying an electric potential to polymer solutions [13]. In low-viscosity liquids, the fluid forms a Taylor Cone at the capillary tip instead of dripping, emitting a charged jet that undergoes Coulomb fission upon solvent evaporation. In polymer solutions, a sufficient emitter-collector distance enables solvent evaporation, yielding micro- and nanoscale spherical particle deposition.

Key phenomena include charge migration to the liquid surface, which creates an electric-field discontinuity, inducing electrostatic pressure that deforms the liquid surface. While surface tension typically balances this pressure, excessive fields cause large-scale deformation. Experimental observations confirm Taylor Cone formation (Figure **1**), validating the electrostatic suction-surface tension equilibrium [16].

Figure 1: Taylor cone generated during an electrospraying process. Taken from [17].

2.2. Material and Equipment

The following materials were used for this electrospraying project:

- Solution Preparation

1. Polyvinyl Alcohol (PVA): Sigma-Aldrich (225 g, Mw: 89000 – 98000, 99% hydrolyzed, CAS: 9002-89-5).
2. Polyvinylpyrrolidone (PVP): Sigma-Aldrich (225 g, Mw: 40000, K-Value 29-32, CAS: 9003-39-8).
3. Deionized Water: Karal (1320 mL, conductivity ≤1.5 µS/cm, pH 5.0-7.0, CAS: 7732-18-5).
4. Absolute Ethanol: Karal (660 mL, ≥99.5% purity, CAS: 64-17-5).
5. Analog/Digital Hotplate Stirrers: Anzeser SH-2 (100 rpm – 2 000 rpm, 350°C) [28] and Joanlab HS5S (50 rpm – 1500 rpm, 310°C).
6. Electronic Balance: Velab VE-1000 (1 000 g capacity, ±0.01 g accuracy).

- Electrospraying Process

1. Electrospinning device: BioiniciaFluidnatek LE-100 (0kV - 30 kV).
2. Syringes: B. Braun Norm-JectLuer Solo (10 mL, DEHP-free).
3. Safety Equipment: Nitrile gloves, lab coat, KF94 mask

- Characterization

1. Optical Microscope: LabomedCxL (4X-100X objectives, LED illumination).
2. Conductivity Meter: Jyving E-1 (0 µS/cm – 9 999 µS/cm, ±2% accuracy).

2.3. Solution Preparation and Conductivity Measurement

The scientific method [34] was employed to develop nine duplicate solutions: six with PVP and three with PVA at varying concentrations in deionized water and absolute ethanol. All procedures were conducted in the Mechanical-Electrical Engineering Laboratory at Universidad Veracruzana, Poza Rica-Tuxpan campus.

- Preparation Protocol

1. Weighing: Polymers (PVA/PVP) were weighed using a Velab electronic balance (VE-1000, ±0.01 g accuracy) after 20-second stabilization.
2. Mixing: Solutions (100 mL each) were prepared using:
3. Joanlab HS5S digital stirrer (primary solutions, 700 rpm).
4. Anzeser SH-2 analog stirrer (duplicates, 60°C).
5. Two Kimax borosilicate beakers (250 mL, ASTM E960).
6. Temperature Control: Maintained at 60°C(monitored with Brannan LAB-025 thermometer, ±1°C accuracy) during 10-minute mixing.

- Solution Compositions

1. Aqueous PVA: 10%, 12.5%, 15% w/v in deionized water.
2. Aqueous PVP: 10%, 12.5%, 15% w/v in deionized water
3. Alcoholic PVP: 10%, 12.5%, 15% w/v in absolute ethanol

(Concentrations selected based on prior electrospraying literature [13]).

- Conductivity Measurement

1. Post-preparation, conductivity was measured using a Jyving E-1 meter (0 µS/cm – 9 999 µS/cm range, ±2% accuracy).
2. Figure **2** shows the manufacturing process for PVA and PVP solutions, using equipment such as a magnetic stirrer, an electronic scale, and a conductivity meter.

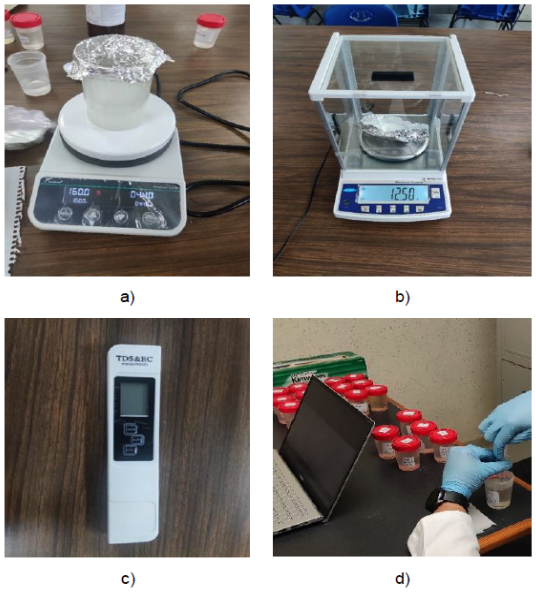

Figure 2: Preparation of PVA and PVP solutions using a) magnetic stirrer, b) electronic scale, and c) conductivity meter.

- Viscosity Measurement

1. Viscosity measurements were performed using AMETEK Brookfield DV-2 (Accuracy ±1.0% of range, repeatability: ±0.2%).

2.4 Electrospraying Processing

The solutions were processed using a Fluidnatek LE-100 electrospraying system (Bioinicia) at the Nanobiotechnology Laboratory (MICRONA Research Center) as shown in Figure **3**.

- Experimental Setup

Initial Parameters:

1. Voltage: 20 kV.
2. Flow rate: 50 µL/h.
3. Collector distance: 18 cm.
4. Solutions: PVA/PVP in deionized water/ethanol (10% – 15% w/v), excluding 15% aqueous PVA due to risk of clogging.

- Environmental Control:

1. Temperature: ≤24°C
2. Relative humidity: ≤44% (monitored via HTC-1 thermohygrometer), conditions critical to prevent electrospraying instability [13].

- Process Workflow:

1. Sample Loading: 4 mL of each solution loaded into B. Braun Norm-Ject syringes.
2. Substrate Preparation: Aluminum foil-covered collector for sample deposition.
3. Parameter Optimization: Iterative adjustments (±kV, ±µL/h, ±cm distance) with 3 min – 5 min stabilization intervals per test.

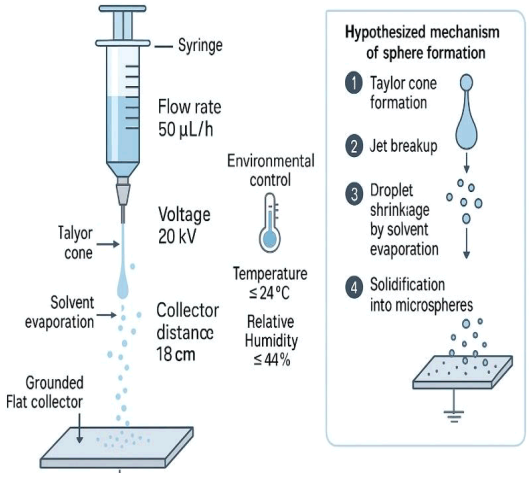

Figure 3: Schematic diagram illustrating the electrospraying setup.

Structure Confirmation via Optical Microscopy

Following electrospraying trials at MICRONA, samples deposited were analyzed using a LabomedCxL binocular optical microscope [32] to verify nanostructure formation.

- Protocol:

Imaging Parameters:

40X magnification (LP DIN semi-plan achromatic objective).

LED illumination (intensity-adjusted).

- Validation Method:

Three independent observations per sample.

Comparative assessment against expected morphologies from literature [13].

- Outcome:

Microscopic analysis confirmed the presence of electrosprayed structures.

3. RESULTS AND DISCUSSIONS

3.1. Solution Preparation and Conductivity Analysis

The conductivity of prepared polymer solutions was systematically quantified, with aqueous PVA solutions exhibiting values of 450 µS/m (10% w/v), 510 µS/m (12.5%), and 470–590 µS/m (15%). (see Table **1**).Duplicate measurements showed <5% variance (e.g., 450 µS/m vs. 470 µS/m for 10% PVA), confirming preparation consistency. PVP solutions in deionized water demonstrated higher conductivities (482 µS/m–586 µS/m) than PVA equivalents at matched concentrations, attributed to PVP's pyrrolidone groups, which enhance ionic mobility [25]. In contrast, PVP/ethanol solutions yielded significantly lower conductivities (44µS/m –56 µS/m), reflecting ethanol's dielectric suppression of charge transport [13].

- Solvent Dependence:

1. Aqueous solutions exceeded 450 µS/m, satisfying the 100 µS/m minimum threshold for stable electrospraying.
2. Ethanol-based solutions remained below 60 µS/m, suggesting potential need for conductivity enhancers (e.g., salts) in future work.

- Concentration Effects:

1. Non-monotonic changes in conductivity (e.g., 506 µS/m at 12.5% vs. 580 µS/m at 15% PVA) indicate competing polymer chain entanglement and charge-carrier mechanisms.
2. PVP's 12.5% aqueous solutions showed peak conductivity (536±3 µS/m), proposing an optimal concentration window.

These results align with electrospraying literature, where conductivities >100 µS/m typically enable Taylor Cone stability [13]. The low ethanol solution values may explain the observed jetting instabilities during trials. The minimal variance between duplicates (<8 µS/m across all systems) validates the reproducibility of the preparation protocol.

3.2. Electrospraying test result

The electrospraying process window was systematically mapped through an iterative parameter optimization. Initial conditions were based on literature values for PVA (20 kV, 50 µL/h, 18 cm) [22-13], from which flow rate (10 µL/h–82 µL/h), applied voltage (20 kV–30 kV), and nozzle-collector distance (8 cm–18 cm) were varied sequentially. The optimization aimed to achieve a stable Taylor Cone (Figure **4**) and then transition to a consistent, drip-free spray for droplet deposition. From the 32 trials conducted, only two parameter sets met all success criteria for their respective polymers, as summarized in Table **2** and visualized in the process optimization space (Figure **5**).

1.3. Statistical Analysis of Conductivity Data

Since the conductivity data follow a normal distribution (Anderson-Darling Test p > 0.05), a

Table 1: Conductivity and Viscosity Obtained from Working Solutions (1) and Duplicates (2)

Polymer	Solvent	Concentration (%)	Conductivity (µS/m)	Viscosity (cP)
PVA	Deionizedwater	10.0	460±10	241±2
		12.5	506±4	1603±6
		15.0	580±10	5925±8
PVP		10.0	480±2	117±5
		12.5	533±3	145±2
		15.0	570±6	176±1
PVP	Absoluteethyl alcohol	10.0	46±2	135±6
		12.5	51±2	181±3
		15.0	54±2	758±3

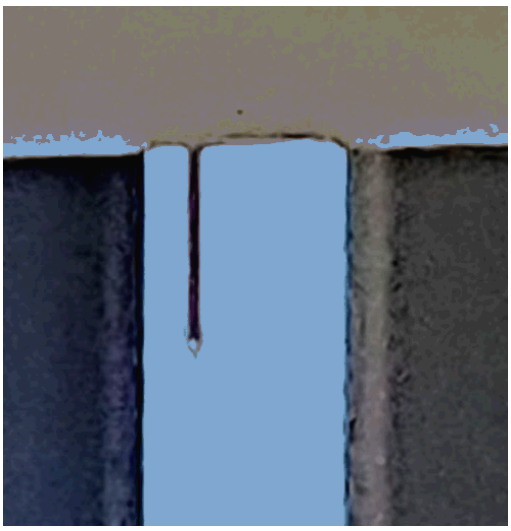

Figure 4: Taylor cone, obtained in tests carried out at Microna (sharpness increased to 50%).

Table 2: Successful tests Solutions Considered Acceptable for the Electrospraying Process

Test	Polymer	Solvent	Concentra-tion (%)	Flowrate (µL/h)	Volt (kV)	Nozzle-collectordistance (cm)
14	PVA	Deionizedwater	10	20	25	12
32	PVP		15	10	30	14

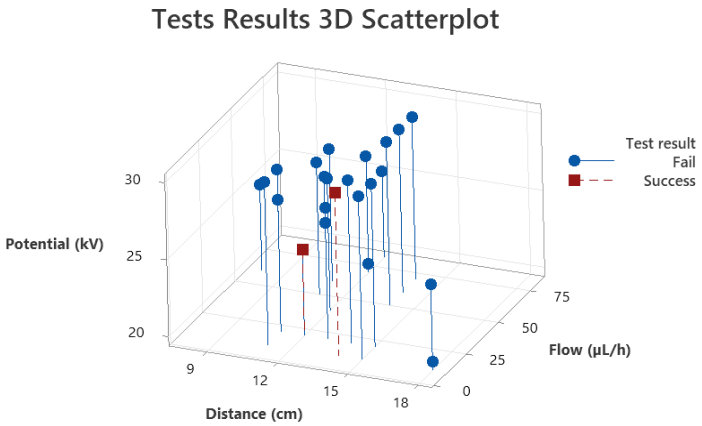

Figure 5: Summary graphic of test results.

two-way ANOVA was conductedto assess the effects of polymer type (PVA vs. PVP) and concentration (10%–15% w/v) on solution conductivity. The results observed in Figure **6**, revealed a statistically significant interaction between these factors ($p < 0.05$), indicating that the effect of concentration on conductivity depends fundamentally on the polymer used.

This interaction can be interpreted in terms of the distinct chemical architectures of the two polymers. PVP, with its polar pyrrolidone group, offers a higher density of sites for ion dissociation and transport compared to the hydroxyl groups of PVA [18]. Consequently, increasing the PVP concentration (Figure **6**) consistently increases the availability of charge carriers, resulting in a monotonic rise in conductivity. In contrast, PVA's behavior is non-monotonic; the initial conductivity increase at 12.5% w/v is likely offset at 15% w/v by the dominant effect of chain entanglement and increased viscosity, which hinders ion mobility—a phenomenon near PVA's gelation threshold reported elsewhere [19].

Afterwards, an interaction differences test was conducted. A total of 15 contrasts were obtained, and the results showed that conductivity was higher with the combination of the polymer PVP at 12.5% or 15%.

The optimal conditions for electrospraying assured a conductivity >450 µS/m, enabling Taylor Cone stability [25] at moderate flow rates between 10 µL/h and 20 µL/h with a balanced jet formation vs. droplet aggregation [22]. The selection of PVP and its superior performance align with its higher conductivity (570 µS/m at 15%) and lower viscosity at equivalent concentrations vs PVA.

Table 3: Interaction, Main Effects Result, and Contrasts from the Two-way ANOVA. A= Concentration, B= Polymer

	Sum sq	Mean Sq	F value	P value
A	7065	3532	22.03	0.0017*
B	6440	6440	40.17	0.0007*
A*B	2873	1436	8.958	0.0157*

*Significant at α=0.05

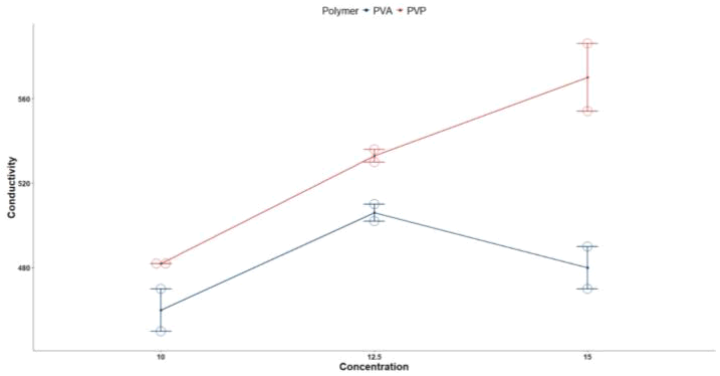

Figure 6: Interaction plot of the main effects Polymer vs Concentration.

The polymer-concentration interaction (p = 0.016) underscores the need for material-specific parameter optimization in electrospraying systems.

3.4. Optical Microscopy Validation

Optical microscopy analysis confirmed the successful formation of structures in the 10% PVA aqueous solution processed at 20 µL/h, 25 kV, and a collector distance of 12 cm (see Figure **7**). The observed morphology validates the electrospraying parameters, though the resolution limit of optical microscopy prevented precise size measurement of the generated structures. Environmental sensitivity was evident, as the 15% PVP solution degraded before characterization due to solvent evaporation during transport, reinforcing the need for strict humidity control (RH ≤44%) during sample handling. These structures demonstrate potential for textile industry applications, particularly as functional coating additives or controlled-release carriers, though nanoscale characterization via SEM would be required for complete morphological analysis. The results substantiate that stable Taylor Cone formation directly correlates with successful particle generation when ambient conditions are properly maintained.

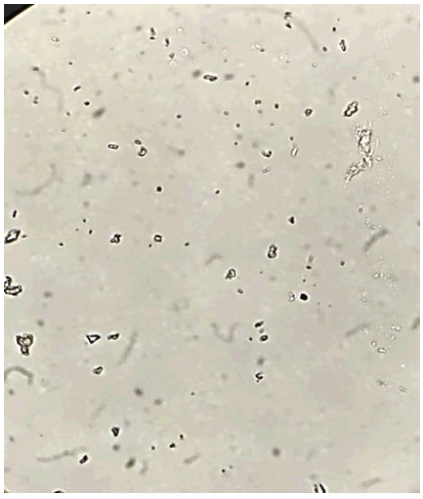

Figure 7: Structures confirmed through optical microscopy.

The systematic optimization revealed distinct electrospraying windows for PVA and PVP, governed by the interplay of solution properties, process parameters, and polymer-specific behavior.

3.5 Solvent Selection and Conductivity

The stark contrast in performance between aqueous and ethanolic solutions is primarily attributable to dielectric and evaporative properties. The high dielectric constant of water (~80.1 at 20°C) facilitates greater charge dissociation, yielding conductivities (>450 µS/m) sufficient for Taylor cone stabilization [20]. In contrast, ethanol's lower dielectric constant (~24.5) and conductivity (<60 µS/m) result in insufficient charge density at the jet surface, leading to unstable jetting and failed spray formation [21]. Furthermore, ethanol's high volatility likely led to premature polymer precipitation or viscosity instability at the needle tip, preventing consistent jet formation [22].

3.6. Polymer-Specific Behavior and Concentration Dependence

The significant polymer-concentration interaction (p = 0.016) underscores fundamentally different structure-property relationships. PVP's consistent

increase in conductivity with concentration aligns with its role as a charge-carrying polymer, where higher solid content provides more ionic transport sites without a drastic increase in viscosity in the studied range [23]. Conversely, the non-monotonic conductivity and processability failure of PVA at 15% w/v points to a competition between charge carriers and rheological percolation. Near this concentration, PVA chains in water begin to form a transient network, leading to a sharp, nonlinear increase in viscosity and elastic modulus that hinders jet elongation and promotes capillary clogging [24]. This explains why only the 10% PVA solution, with a more favorable viscosity-conductivity balance, was successfully processed.

Parametric Optimization and Process Window

The optimal parameters (10% PVA at 20 µL/h, 25 kV, 12 cm, and 15% PVP at 10 µL/h, 30 kV, 14 cm) define a narrow, material-specific process window. The lower flow rate required for PVP (10 µL/h vs. 20 µL/h for PVA) correlates with its higher conductivity, as a lower volumetric flow is needed to achieve the same charge density for jet fission [25]. The higher optimal voltage for PVP (30 kV) further compensates for its potentially higher solution viscosity at 15% concentration, thereby maintaining electrostatic pulling forces. These results empirically confirm that universal electrospraying parameters are unfeasible; optimization must account for the unique physicochemical signature of each polymer-solvent system [22,25].

4. CONCLUSION

This study experimentally determined the operational parameters for generating structures via electrospraying from aqueous PVA and PVP solutions using a Fluidnatek LE-100 system. The results demonstrate that process feasibility critically depends on a specific combination of polymer, solvent, and process parameters.

Two optimal condition sets enabling stable Taylor Cone formation and sphere generation were identified: 10% w/v aqueous PVA solutions (20 µL/h, 25 kV, 12 cm) and 15% w/v aqueous PVP solutions (10 µL/h, 30 kV, 14 cm). In contrast, formulations with absolute ethanol did not produce a stable electrospray across the tested concentration range (10%-15%), attributed to their low conductivity (<60 µS/m) and high evaporation rate. Furthermore, the 15% PVA solution was untreatable due to a significant increase in viscosity, leading to clogging.

Statistical analysis confirmed that the effect of concentration on solution conductivity differs significantly across polymers ($p = 0.016$), underscoring the need for material-specific parameter optimization.

While the long-term goal is to apply these polymeric structures as photocatalyst carriers in textile wastewater treatment, the core contribution of this work is to establish a reproducible, quantitative protocol for generating the base spheres. The optimal parameters reported here constitute the essential foundational step for future research aimed at functionalizing these estructures with TiO2 and evaluating their photocatalytic activity.

AUTHOR CONTRIBUTIONS

All authors contributed to manuscript writing, reviewing and editing, to the final version for submission.

REFERENCES

[1] Fenn JB, Mann M, Meng CK, Wong SF, Whitehouse CM. Electrospray ionization for mass spectrometry of large biomolecules. Science 1989; 246(4926): 64-71. https://doi.org/10.1126/science.2675315

[2] Bartoli C, von Rohden H, Thompson SP, Bloomers J. A liquid caesium field ion source for space propulsion. Journal of Physics D: Applied Physics 1984; 17(12). https://doi.org/10.1088/0022-3727/17/12/014

[3] Gautam A, Clifford WJ, Densmore CL. Aerosol gene therapy. Mol Biotechnol 2003; 23: 51-60. https://doi.org/10.1385/MB: 23: 1: 51

[4] Deitzel JM, Kleinmeyer JD, Harris D, Beck-Tan NC. The effect of processing variables on the morphology of electrospun nanofibers and textiles. Polymer 2001; 42(1): 261-272. https://doi.org/10.1016/S0032-3861(00)00250-0

[5] González Molfino HM, Alcalde Yañez A, Valverde Morón VV, Villanueva Salvatierra DV. Electrospinning: Advances and applications in the field of biomedicine. Revista de la Facultad de Medicina Humana 2020; 20(4): 706-713. https://doi.org/10.25176/RFMH.v20i4.3004

[6] Sánchez Fuentes A. Electrospinning vs Electrospraying para la optimización de los parámetros de deposición en el diseño de recubrimientos nanoestructurados de uso biomédico. Trabajo de fin de grado. Pamplona: Universidad Pública de Navarra, E.T.S de Ingeniería Industrial, Informática y de Telecomunicación; 2022.

[7] Zafar M, Najeeb S, Khurshid Z, Vazirzadeh M, Zohaib S, Najeeb B, et al. Potential of Electrospun Nanofibers for Biomedical and Dental Applications. Materials 2016; 9(73). https://doi.org/10.3390/ma9020073

[8] Haider A, Haider S, Kang IK. A comprehensive review summarizing the effect of electrospinning parameters and potential applications of nanofibers in biomedical and biotechnology. Arabian Journal of Chemistry 2018; 11: 1165-1188. https://doi.org/10.1016/j.arabjc.2015.11.015

[9] Kamoun EA, Kenawy ERS, Chen X. A review on polymeric hydrogel membranes for wound dressing applications: PVA-based hydrogel dressings. J Adv Res 2017; 8(3): 217-233. https://doi.org/10.1016/j.jare.2017.01.005

[10] Ramírez A, Benitez JL, Rojas de Astudillo L, Rojas de Gáscue B. Materiales polimeros de tipo hidrogeles: revisión sobre su caracterización mediante ftir, dsc, meb y met. Revista Latinoamericana de Metalurgia y Materiales 2016; 36(2).

[11] Deitzel JM, Kleinmeyer J, Harris D, Beck Tan NC. The effect of processing variables on the morphology of electrospun nanofibers and textiles. Polymer 2001; 42(1): 261-272. https://doi.org/10.1016/S0032-3861(00)00250-0

[12] Buwalda SJ, Boere KWM, Dijkstra PJ, Feijen J, Vermonden T, Hennink WE. Hydrogels in a historical perspective: From simple networks to smart materials. J Control Release 2014; 190: 254-73. https://doi.org/10.1016/j.jconrel.2014.03.052

[13] Schmatz AD, Vieira Costa JA, Joanol da Silveira Mastrantonio D, Greque de Morais M. Encapsulation of phycocyanin by electrospraying: A promising approach for the protection of sensitive compound. Food and Bioproducts Processing 2020; 119: 206-215. https://doi.org/10.1016/j.fbp.2019.07.008

[14] Lei L, Zhaoyang L, Bai H, Sun DD. Concurrent filtration and solar photocatalytic disinfection/degradation using high-performance Ag/TiO2 nanofiber membrane. Water Research 2012; 46(4): 1101-1112. https://doi.org/10.1016/j.watres.2011.12.009

[15] Hassen T, Grah PA, Olfa H, Yehe DM, Didier R, Patrick D, et al. Solar Photocatalytic Decolorization and Degradation of Methyl Orange. J. Adv. Oxid. Technol 2016; 19(1). https://doi.org/10.1515/jaots-2016-0110

[16] GI. Disintegration of water drops in an electric field. Royal Society 1964; 280(1382). https://doi.org/10.1098/rspa.1964.0151

[17] Morad MR, Rajabi A, Razavi M, Pejman Sereshkeh SR. A Very Stable High Throughput Taylor Cone-jet in Electrohydrodynamics. Scientific Reports 2016: 3. https://doi.org/10.1038/srep38509

[18] Shao J, Zhao Y, Wu Y, Xue Q. Recent progress in the synthesis of polyvinylpyrrolidone and its applications in batteries, sensors, and capacitors. J Mater Chem A 2020; 8(46): 24175-24203.

[19] Teodorescu M, Bercea M, Morariu S. Biomaterials of PVA and PVP in medical and pharmaceutical applications: Perspectives and challenges. Biotechnol Adv 2019; 37(1): 109-131. https://doi.org/10.1016/j.biotechadv.2018.11.008

[20] Rayleigh L. On the equilibrium of liquid conducting masses charged with electricity. Philos Mag 1882; 14(87): 184-6. https://doi.org/10.1080/14786448208628425

[21] Jaworek A, Sobczyk AT. Electrospraying route to nanotechnology: An overview. J Electrostat 2008; 66(3-4): 197-219. https://doi.org/10.1016/j.elstat.2007.10.001

[22] Cloupeau M, Prunet-Foch B. Electrohydrodynamic spraying functioning modes: a critical review. J Aerosol Sci 1994; 25(6): 1021-36. https://doi.org/10.1016/0021-8502(94)90199-6

[23] Zhang S, Campagne C, Salaün F. Influence of solvent selection in the electrospraying process of polycaprolactone. Appl Sci 2019; 9(3): 402. https://doi.org/10.3390/app9030402

[24] Teodorescu M, Bercea M, Morariu S. Biomaterials of PVA and PVP in medical and pharmaceutical applications: Perspectives and challenges. Biotechnol Adv 2019; 37(1): 109-31. https://doi.org/10.1016/j.biotechadv.2018.11.008

[25] Hartman RPA, Brunner DJ, Camelot DMA, Marijnissen JCM, Scarlett B. Electrohydrodynamic atomization in the cone-jet mode physical modeling of the liquid cone and jet. J Aerosol Sci 1999; 30(7): 823-49. https://doi.org/10.1016/S0021-8502(99)00033-6

Received on 07-11-2025 Accepted on 06-12-2025 Published on 22-12-2025

https://doi.org/10.6000/1929-5995.2025.14.22